BULLETIN OF THE POLISH ACADEMY OF SCIENCES
TECHNICAL SCIENCES, Vol. 69(2), 2021, Article number: e136725
DOI: 10.24425/bpasts.2021.136725

SPECIAL SECTION
Machine modelling and simulations

Axial stiffness for large-scale ball slewing rings with four-point contact

Slavomir HRCEK[1], Robert KOHAR[1], and Jan STEININGER[2]

[1] University of Zilina, Faculty of Mechanical Engineering, Department of Design and Machine Elements, Slovak Republic
[2] University of Zilina, Institute of Competitiveness and Innovations, Slovak Republic

Abstract. This article deals with the design of slewing rings (slewing bearings). A fully parametric, 3D virtual model of a ball slewing ring with four-point contact was created in the PTC/Creo Parametric CAD system. This model was subsequently used for finite-element analysis using Ansys/Workbench CAE software. The purpose of the FEM analysis was to determine the axial stiffness characteristics. Results of FEM analysis were experimentally verified using a test bench. At the end of the article, we present the nomograms of the deformation constant for different pitch diameters, rolling element diameters and contact angles.

Key words: stiffness; experimental measurement; slewing ring; deformation constant.

1. Introduction

Rolling bearings are one of the fundamental structural components of all machinery and equipment. Their service life depends mainly on the size of the load, respectively on the magnitude of the contact stress state that exists between the rolling elements and the orbital path of the bearing rings (races) transferring the external load.

Slewing rings are actually a special type of rolling bearings. According to the rolling elements used, slewing bearings are divided into ball slewing rings (with one or two rows of rolling elements) and roller slewing rings of two types: crossed roller slewing rings, and combined (radial-axial) rings. They can be considered as large-dimensional ball bearings with angular contact transferring the dominant axial load or tilting moment.

The currently known generalized constants derived in the past to calculate the stiffness of rolling bearings do not ensure sufficient accuracy when calculating stiffness for larger slewing ring dimensions (diameters exceeding 2.5 meters).

It is therefore desirable to determine a stiffness constant for different dimensional series. Using virtual 3D models and FEM simulation, it is possible to theoretically determine the characteristics of axial stiffness based on the displacements and forces acting between the rolling elements and race orbital paths. Subsequently, it is possible to analytically determine a deformation constant, which needs to be verified experimentally.

2. Literature Review

Studies on rolling element bearings were performed by Guo and Parker [1], Chen and Wang [2]. They investigated the non-linear relation between bearing deflection and applied load. Gargiulo gives empirical formulae for the load-stiffness and deflection-stiffness relations by assuming rigid bearing races. These formulae apply for radial and axial stiffnesses for a few bearing types [3, 4].

The design of slewing rings requires the knowledge of what internal forces act between the rolling elements and the orbital paths, and thus knowing the contact stress state between them [5, 6].

Hertz established relationships to calculate the contact stress state between bodies with different curvature of contact surfaces. He also defined relationships to calculate stiffness for point contact and line contact [7].

In general, calculation of the contact stress state (or the force action between rolling elements and the race orbital paths) depends, in particular, on stiffness. The rolling bearing stiffness is characterized by the amount of elastic deformation of the rolling bearing under load. Stiffness is expressed as the load-to-deformation ratio and depends on a number of parameters, such as the number and size of the rolling elements, geometric dimensions of the race orbital paths, contact angle, pre-stress, and others [8].

Currently, generalized constants derived in the past to calculate the stiffness of rolling bearings are known for all sizes, but these constants do not ensure sufficient accuracy when calculating larger rolling bearing stiffness. For instance, Kurvinen et al. [9] increased the complexity of a numerical model of ball bearings to study the effect of the rotation speed, centrifugal and gyroscopic forces and bearing stiffness coefficient on the bearing performance. However, today's trend in this area includes large-dimensional slewing rings exceeding 2.5 meters in diameter. Their correct and effective design requires determination of these stiffness constants in the simplest way possible.

In general, axial stiffness is expressed by the relationship between the axial force Fa and the axial deformation δa. Assume that only the axial load acts on the slewing ring, namely

*e-mail: robert.kohar@fstroj.uniza.sk

Manuscript submitted 2020-08-21, revised 2021-01-26, initially accepted for publication 2021-02-22, published in April 2021

© 2021 The Author(s). This is an open access article under the CC BY license (http://creativecommons.org/licenses/by/4.0/).

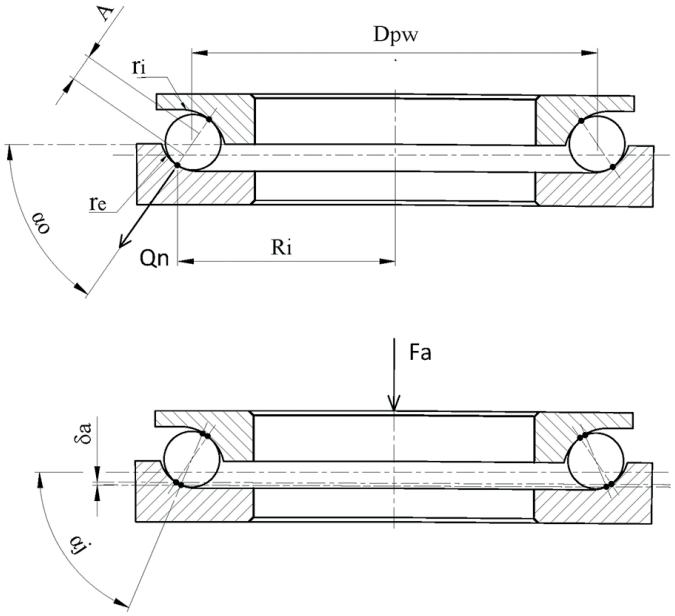

Fig. 1. Auxiliary geometry parameters

on the inner race (the outer race is firm), as shown in Fig. 1. The greater the axial force Fa, the greater the displacement of the inner race against the outer race, hence the greater axial deformation δa.

The most appropriate way to determine the axial stiffness of (in this case) ball slewing rings is using finite-element analysis [10, 11]. However, this analysis needs to be verified by experimental measurement, given the correctness of their settings (boundary conditions, setting of contact parameters between the rolling elements and the race orbital paths) and the relevance of the results obtained. Royston and Basdogan [12] measured radial and axial stiffnesses of a self-aligning ball bearing with combined radial and axial preloads. Bogard et al. [13] used numerical determination of the mechanical stiffness of a force measurement device based on capacitive probes. Walford and Stone [14] developed a test rig to measure the radial stiffness of a pair of angular contact ball bearings under oscillating conditions.

Parametric studies were further conducted to identify the effects of lubricant temperature, rotor speed, and applied load on this bearing pair. Recently, techniques to experimentally determine bearing dynamic coefficients were developed through vibratory response measurements of rotor-bearing systems. Tiwari et al. [15] used identification techniques to estimate certain dynamic bearing stiffnesses from unbalance and impulse response measurements of rotor-bearing test rigs. Goodwin [16] reviewed the experimental approaches to identify bearing stiffness and damping. Relationships for the calculation of the deformation constant c_δ will be mathematically derived after verifying the accuracy of the calculated results from FEM analysis by experimental measurement, using special test equipment for large-dimensional rolling bearings and validate the proposed stiffness determination method by comparing results against published experiments [17].

Hertz's relationship can be used to calculate elastic deformation in order to analytically express the ball slewing ring stiffness. Elastic deformation δ_n is calculated, according to Hertz`s theory, separately for each point of contact, i.e., it is calculated separately for the rolling element – inner race contact, and separately for the rolling element – outer race contact. For two bodies with point contact consisting of the same material and subjected to a compression force Q_n (N), Hertz calculates deformation as [18]:

$$\delta_n = 1.5\left(\frac{2K}{\pi\mu}\right)\sqrt[3]{\left(\frac{1-u^2}{E}\right)^2\left(\frac{\sum\rho}{3}\right)Q_n^2}\,, \tag{1}$$

if the effective elastic modulus is [19]:

$$E' = \frac{E}{(1-u^2)}, \tag{2}$$

then Eq. (1) can be written as:

$$\delta_n = 1.5\left(\frac{2K}{\pi\mu}\right)\sqrt[3]{\left(\frac{1}{E'}\right)^2\left(\frac{\sum\rho}{3}\right)Q_n^2}\,, \tag{3}$$

from Eq. (3) the constant K is introduce:

$$K = 1.5\sqrt[3]{\frac{1}{3}}, \tag{4}$$

simplified and modified relationship is obtained:

$$\delta_n = K\left(\frac{2K}{\pi\mu}\right)\sqrt[3]{\left(\frac{1}{E'}\right)^2\sum\rho Q_n^2}\,. \tag{5}$$

The total elastic deformation δ_n for rolling bearings or slewing rings is then equal to the sum of the elastic deformation δ_i between the inner race and the rolling element, and the elastic deformation δ_o between the rolling element and the outer race:

$$\delta_n = \delta_i + \delta_o. \tag{6}$$

Then the total elastic deformation is equal to:

$$\delta_n = K\left(\frac{2K}{\pi\mu_i}\right)\sqrt[3]{\left(\frac{1}{E'}\right)^2\sum\rho_i Q_n^2} + K\left(\frac{2K}{\pi\mu_o}\right)\sqrt[3]{\left(\frac{1}{E'}\right)^2\sum\rho_o Q_n^2}\,. \tag{7}$$

After formal adjustments it is obtained:

$$\delta_n = K\left(\frac{2K}{\pi\mu_i}\right)\left(\frac{1}{E'}\right)^{\frac{2}{3}}\left(\sum\rho_i\right)^{\frac{1}{3}}(Q_n)^{\frac{2}{3}} + \\ + K\left(\frac{2K}{\pi\mu_o}\right)\left(\frac{1}{E'}\right)^{\frac{2}{3}}\left(\sum\rho_o\right)^{\frac{1}{3}}(Q_n)^{\frac{2}{3}}. \tag{8}$$

By adjusting the magnitude of the constant K to:

$$K = 2*1.5\sqrt[3]{\frac{1}{3}}. \tag{9}$$

Then it is possible to modify Eq. (10) if it is necessary to express the magnitude of the normal force Q_n acting on:

$$\delta_n^{\frac{2}{3}} = K^{\frac{2}{3}}\frac{1}{E'}Q_n\left[\frac{2K}{\pi\mu_i}\left(\sum\rho_i\right)^{\frac{1}{3}} + \frac{2K}{\pi\mu_o}\left(\sum\rho_o\right)^{\frac{1}{3}}\right]^{\frac{3}{2}}, \tag{10}$$

$$K = 1.5\sqrt[3]{\frac{1}{3}}, Q_n = \delta_n^{\frac{3}{2}}\frac{E'}{K^{\frac{3}{2}}\left[\frac{2K}{\pi\mu_i}\left(\sum\rho_i\right)^{\frac{1}{3}} + \frac{2K}{\pi\mu_o}\left(\sum\rho_o\right)^{\frac{1}{3}}\right]^{\frac{3}{2}}}. \tag{11}$$

If the constant c_δ is introduced for the contact of three bodies with a spherical surface from point to point:

$$c_\delta = \frac{E'}{K^{\frac{3}{2}}\left[\frac{2K}{\pi\mu_i}\left(\sum\rho_i\right)^{\frac{1}{3}} + \frac{2K}{\pi\mu_o}\left(\sum\rho_o\right)^{\frac{1}{3}}\right]^{\frac{3}{2}}}. \tag{12}$$

The relation for the normal force Q_n is obtained in the following well-known form [19]:

$$Q_n = c_\delta\delta_n^{\frac{3}{2}}. \tag{13}$$

In the case of axially loaded bearings, it is rather necessary to deal with the axial deformation δ_a, which is caused by the external loading axial force F_a. The relationship between the axial deformation δ_a and the normal deformation δ_n can be expressed using the goniometric function:

$$\sin\alpha_o = \frac{\delta_a}{\delta_i + \delta_o} = \frac{\delta_a}{\delta_n} \rightarrow \delta_n = \frac{\delta_a}{\sin\alpha_o}, \tag{14}$$

then the resulting relationship between the normal force acting on the rolling element and the axial deformation of the slewing ring will be:

$$Q_n = c_\delta\left(\frac{\delta_a}{\sin\alpha_o}\right)^{\frac{3}{2}}. \tag{15}$$

3. Research Methodology

For FEM analysis, a fully parametric, 3D virtual model of a ball slewing ring with four-point contact was created in the PTC/CreoParametric CAD system. This model was designed so that its geometry was controlled by the parameters through relations. In this way, it is possible to efficiently adjust the individual dimensions and create size-based series of rotating rings. Figure 2 shows a cross-sectional view with the control parameters and relations. In the same manner, Fig. 3 shows the

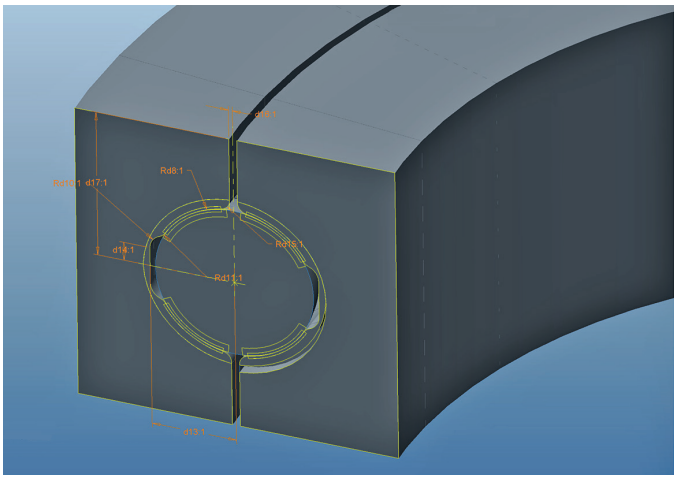

Fig. 2. 3D virtual model of a ball slewing ring with four-point contact with the control parameters and relations

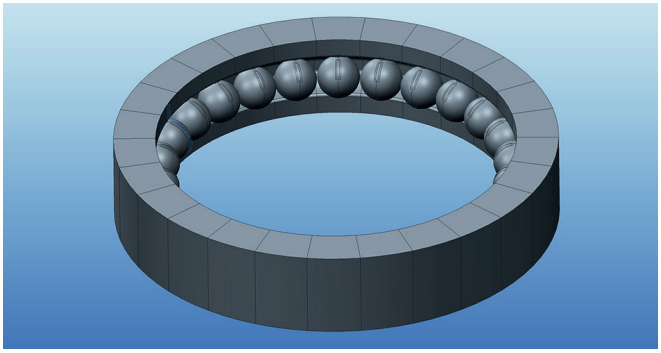

Fig. 3. 3D virtual model of a ball slewing ring with four-point contact – full model

designed full 3D model of a ball slewing ring with four-point contact [20].

The ball slewing ring model was defined by the following basic dimensions:

- rolling elements pitch diameter D_{pw},
- rolling element diameter D_{we},
- contact angle α_0,
- raceway groove radius r_i.

The slewing ring width was defined as twice the rolling element diameter $(B = 2{*}D_{we})$ just like the inner diameter $(d = D_{pw} - 2{*}D_{we})$ and outer diameter $D = D_{pw} + 2{*}D_{we}$. Based on this definition of slewing ring cross-sectional dimensions the corresponding stiffness values were calculated for individual size-based series [21].

Ansys/Workbench CAE software was used to perform the FEM analysis, in which static structural analysis was defined for the ball slewing ring model. The resulting virtual 3D model of a ball slewing ring was imported from the PTC/Creo Parametric system via an interface to the Ansys/Workbench environment. This interface enables us to modify the parameters and thus change the slewing ring model directly from the Ansys/Workbench environment (Fig. 4 – red frame).

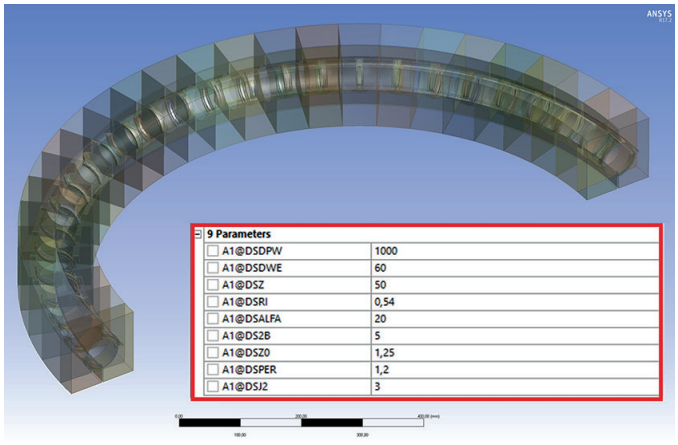

Fig. 4. Ball slewing ring model imported to Ansys/Workbench

For all slewing ring components, a linear isotropic elasticity material model with Young's modulus $E = 210\,000$ MPa and Poisson's ratio $\mu = 0.3$ was used for bearing steels. A linear material model was chosen because such a maximum axial load F_a acting on the slewing ring has developed that it is possible to avoid exceeding the yield strength of the material and the maximum contact pressure exceeding $p_o = 4000$ MPa, which is defined as the threshold value for point contact.

Symmetry was applied to the model in one plane *X–Y* for reducing the computational time. The model mesh (Fig. 5) was created by standard elements from the Ansys library. The volume mesh was created with the *SOLID185* element. Individual bearing elements are in contact because the forces acting upon the bearing are transferred between rings (their raceways) and individual rolling elements. Elements type *CONTA174* and *TARGE170* were used for mesh contact pairs (rolling elements

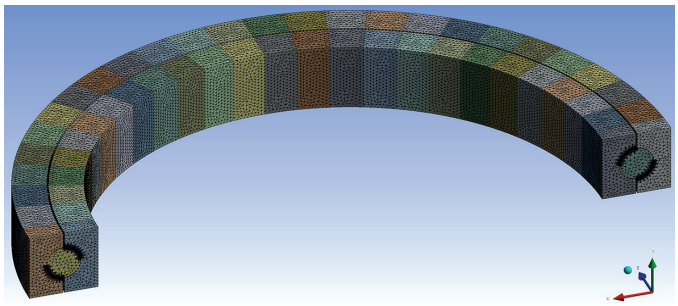

Fig. 5. Finite-element mesh of a ball slewing ring

– raceways). Choosing an appropriate mesh element size is necessary in order to correctly analyze the contact pressure between the roller and roller raceway of the outer and inner rings. The FEM model mesh for contact pressure analysis should be defined by a minimum of 5 elements per half-width of the contact area $b1/2$. Mesh density along the contact profiles has been defined as 3-times the element size along the width of the contact area in order to decrease the finite-element model computational requirements.

The contacts between the rolling elements and orbital paths of the two rings (races) were defined as *Frictional* type with *Coulomb* friction coefficient 0.1 (Fig. 6).

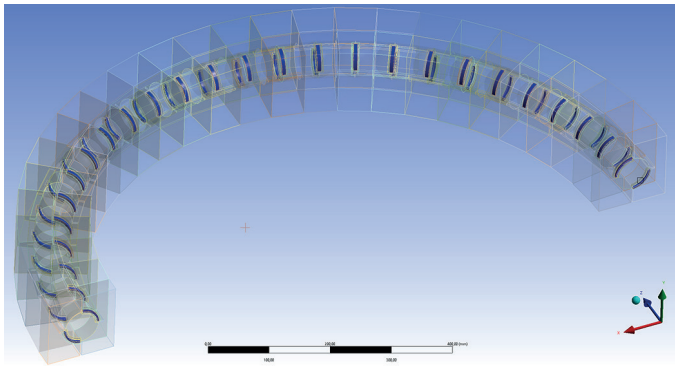

Fig. 6. Definition of Frictional type contacts between the rolling elements and the orbital paths of the races

When calculating axial stiffness, only the elasticity of the ball slewing ring was considered, the surrounding environment was not considered. Boundary conditions and load were defined to represent reality. The position of rolling elements was defined in the cage as in their middle plane, using boundary condition – *frictionless support* (Fig. 7a). Boundary condition displacement for Y-direction was defined on the outer race (Fig. 7b). Axial *force* for Y-direction was defined on the inner race (Fig. 7c) in multiple load-steps to determine the stiffness characteristics of the analysed slewing ring [22].

The purpose of FEM analysis was to determine the axial stiffness characteristics $(Q_n$ vs. $\delta_a)$. In order to determine axial stiffness for individual size-based series of ball slewing rings, we assessed the bearing rings (races) displacement in the axial

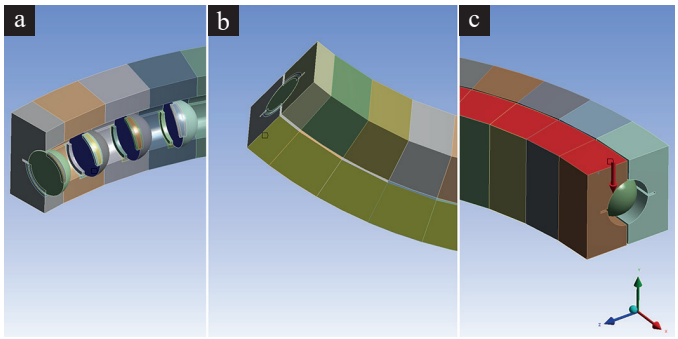

Fig. 7. Definition of boundary conditions and load

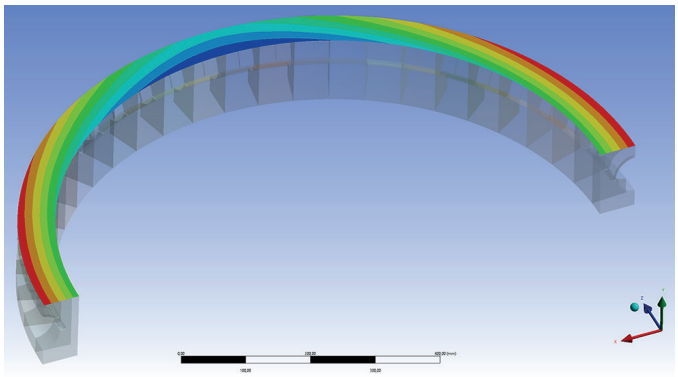

Fig. 8. Assessment of the bearing rings axial displacement δ_a

direction δ_a (Fig. 8) and the magnitude of the force Q_n acting between the rolling elements and the bearing rings (races) orbital paths [23].

Based on the FEM analysis carried out, Table 1 shows the results of axial displacement δ_a which is dependent on the axial load on one rolling element and the ball slewing ring parameters.

The values calculated in the FEM analysis were used to calculate the deformation constant c_δ in an analytical manner for individual size-based series of ball slewing rings, as described in the next paragraph.

4. Experimental verification

The next step was to experimentally verify the carried-out FEM analysis of slewing rings to see if the FEM analysis results correspond to reality. For this purpose, a four-point contact single-row ball slewing ring was selected with the following parameters: rolling elements pitch diameter $D_{pw} = 612$ mm, ball diameter $D_{we} = 30$ mm, contact angle $\alpha_0 = 45°$, and raceway curvature ratio $r_i = 0.5186$ (the ratio of the raceway radius to the ball (rolling element) diameter).

The selected slewing ring to verify the axial stiffness characteristics was used $(F_a$ vs. $\delta_a)$ as compared to the stiffness calculated using the FEM analysis on the designed virtual 3D slewing ring model described in the previous paragraph. In

Table 1
Results of elastic displacement δ_a which is depending on the axial load Q_n on the one rolling element and parameters of the ball slewing ring D_{pw}, D_{we}, α_0 and r_i

		D_{pw} (mm)	500				1000				1500				2000				2500		
α_0	r_i	Q_n*10^3 (N)	2	20	70	85	2	20	70	85	2	20	70	85	2	20	70	85	2	20	32.5
20	0.523	δ_a (mm)	0.1318	0.5453	1.0457	1.1345	0.1985	0.8665	1.5625	1.6561	0.2883	1.2463	2.1699	2.2760	-	-	-	-	-	-	-
20	0.529		0.1421	0.6000	1.1917	1.3034	0.2127	0.9548	1.8342	1.9696	0.3093	1.3758	2.6213	2.7719	-	-	-	-	0.5658	2.3569	2.8818
20	0.535		0.1502	0.6483	1.2475	1.3537	0.2244	1.0326	1.8493	1.9566	0.3268	1.4920	2.6415	2.7741	-	-	-	-	-	-	-
20	0.541		0.1578	0.6914	1.3861	1.5188	0.2350	1.0995	2.1312	2.2744	0.3425	1.5963	2.9817	3.1633	-	-	-	-	0.6379	2.6784	3.2184
20	0.547		0.1649	0.7305	1.4357	1.5650	0.2446	1.1667	2.1522	2.2876	0.3554	1.6915	2.9956	3.1461	-	-	-	-	-	-	-
30	0.523		0.0745	0.3677	0.8258	0.9270	0.1140	0.6288	1.4068	1.5369	0.1705	0.9639	2.0736	2.2345	-	-	-	-	-	-	-
30	0.529		0.0790	0.3955	0.8830	0.9790	0.1200	0.6760	1.4649	1.5994	0.1781	1.0388	2.3187	2.5180	-	-	-	-	0.3595	1.9782	2.5969
30	0.535		0.0832	0.4199	0.9625	1.0876	0.1249	0.7166	1.6577	1.8214	0.1851	1.1030	2.4624	2.6722	-	-	-	-	-	-	-
30	0.541		0.0865	0.4406	1.0004	1.1115	0.1291	0.7521	1.6635	1.8241	0.1940	1.1611	2.6367	2.8758	0.2765	1.6372	3.3059	3.5088	0.3884	2.2199	2.9565
30	0.547		0.0892	0.4594	1.0623	1.1895	0.1327	0.7844	1.7970	1.9852	0.1992	1.2129	2.8127	3.0822	0.2847	1.7142	3.5721	3.7984	0.4018	2.3399	3.1461
40	0.523		0.0496	0.2632	0.6374	0.7271	0.0753	0.4703	1.1707	1.3019	0.1120	0.7563	1.8161	1.9906	-	-	-	-	-	-	-
40	0.529		0.0524	0.2796	0.6757	0.7592	0.0785	0.4970	1.2031	1.3357	0.1169	0.7994	1.9425	2.1341	-	-	-	-	-	-	-
40	0.535		0.0546	0.2937	0.7217	0.8206	0.0815	0.5196	1.3140	1.4730	0.1206	0.8365	2.0616	2.2726	-	-	-	-	0.2505	1.7152	2.3451
40	0.541		0.0575	0.3060	0.7558	0.8677	0.0846	0.5394	1.4099	1.6006	0.1242	0.8696	2.2177	2.4641	0.1802	1.2760	2.9118	3.1382	0.2579	1.8035	2.5163
40	0.547		0.0595	0.3169	0.7864	0.8956	0.0875	0.5575	1.4240	1.5972	0.1285	0.8980	2.3589	2.6525	0.1855	1.3208	3.1923	3.4756	0.2650	1.8753	2.7026
50	0.523		0.0371	0.1999	0.5009	0.5715	0.0559	0.3661	0.9569	1.0677	0.0820	0.6110	1.5288	1.6786	-	-	-	-	-	-	-
50	0.529		0.0395	0.2112	0.5282	0.5970	0.0586	0.3832	0.9928	1.1095	0.0852	0.6378	1.6907	1.8798	0.1235	0.9599	2.2510	2.4363	-	-	-
50	0.535		0.0418	0.2208	0.5592	0.6392	0.0610	0.3977	1.0672	1.2051	0.0870	0.6603	1.8012	2.0173	-	-	-	-	0.1844	1.4520	2.1038
50	0.541		0.0422	0.2296	0.5819	0.6712	0.0621	0.4102	1.1326	1.2964	0.0901	0.6801	1.8849	2.1250	-	-	-	-	0.1889	1.4984	2.2105
50	0.547		0.0439	0.2370	0.6031	0.6971	0.0638	0.4217	1.1748	1.3542	0.0961	0.6988	1.9562	2.2125	-	-	-	-	0.1982	1.5422	2.2825
60	0.523		0.0295	0.1559	0.3767	0.4162	0.0442	0.2932	0.7301	0.7972	0.0668	0.5080	1.2547	1.3607	-	-	-	-	-	-	-
60	0.529		0.0308	0.1647	0.4075	0.4580	0.0457	0.3057	0.7997	0.8866	0.0683	0.5253	1.3692	1.5035	-	-	-	-	-	-	-
60	0.535		0.0338	0.1719	0.4325	0.4953	0.0487	0.3163	0.8652	0.9733	0.0695	0.5412	1.4601	1.6151	0.1005	0.8340	1.9890	2.1461	0.1463	1.2415	1.7708
60	0.541		0.0346	0.1787	0.4511	0.5189	0.0502	0.3257	0.9062	1.0281	0.0772	0.5557	1.5143	1.6825	0.1098	0.8563	2.0818	2.2551	0.1564	1.2741	1.8498
60	0.547		0.0353	0.1848	0.4665	0.5374	0.0511	0.3344	0.9397	1.0709	0.0792	0.5676	1.5779	1.7640	0.1119	0.8759	2.1796	2.3710	0.1608	1.3049	1.9120
70	0.523		0.0242	0.1104	0.1902	0.1843	0.0359	0.2242	0.4326	0.4457	0.0608	0.4167	0.7792	0.8128	0.0876	0.6388	1.0281	1.0563	-	-	-
70	0.529		0.0247	0.1183	0.2235	0.2218	0.0367	0.2350	0.4964	0.5178	0.0587	0.4323	0.9050	0.9544	0.0874	0.6814	1.2116	1.2573	0.1278	0.9758	1.2195
70	0.535		0.0247	0.1251	0.2503	0.2527	0.0369	0.2438	0.5485	0.5787	0.0641	0.4460	1.0152	1.0795	0.0921	0.7069	1.3844	1.4471	0.1327	1.0444	1.3609
70	0.541		0.0264	0.1300	0.2710	0.2790	0.0386	0.2514	0.5884	0.6250	0.0656	0.4595	1.1272	1.2138	0.0936	0.7260	1.5552	1.6394	0.1344	1.0941	1.4935
70	0.547		0.0258	0.1347	0.2846	0.2958	0.0385	0.2585	0.6195	0.6617	0.0653	0.4693	1.1871	1.2855	-	-	-	-	0.1352	1.1265	1.5659

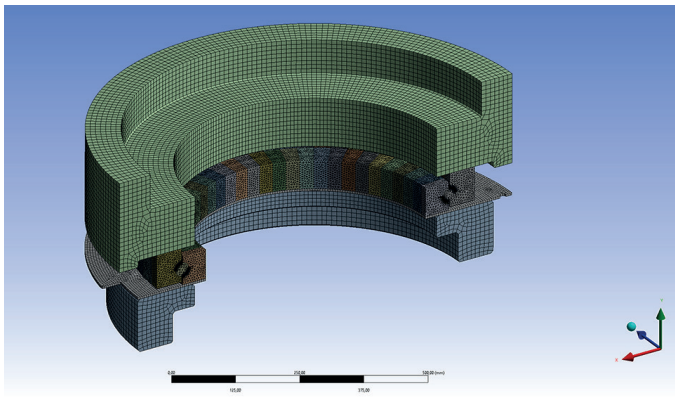

Fig. 9. FEM model of a single-row ball slewing ring with clamping accessories conforming to the testing device conditions

order to compare the FEM analysis results with experimental measurements, it was necessary to complement the slewing ring FEM model with clamping accessories (Fig. 9).

The simulation of the axially loaded slewing ring was calculated, and subsequently the structural analysis results was used (Fig. 10) to assess the displacement of the measuring device (deviation meter) gripping surface in relation to the measured surface (at the touch of the deviation meter tip), which corresponded to the conditions in the experimental test [4].

Experimental measurement was carried out on a special test device for large dimension rolling bearings to verify their service life at a given load. Axial load is drawn between the upper and lower plates through four hydraulic cylinders. The tested rolling bearing or slewing ring is placed between these two plates in clamping accessories. Hydraulic cylinders allow developing a total axial load of 4000 kN.

The slewing ring under test was fixed by clamping accessories and the test device was assembled (Fig. 11). Then, three deviation meters were positioned at selected locations along the slewing ring circumference to measure the magnitude of compression in the axial direction (Fig. 12).

Three independent measurements of axial compression were performed – the bearing rings (races) were rotated relative to

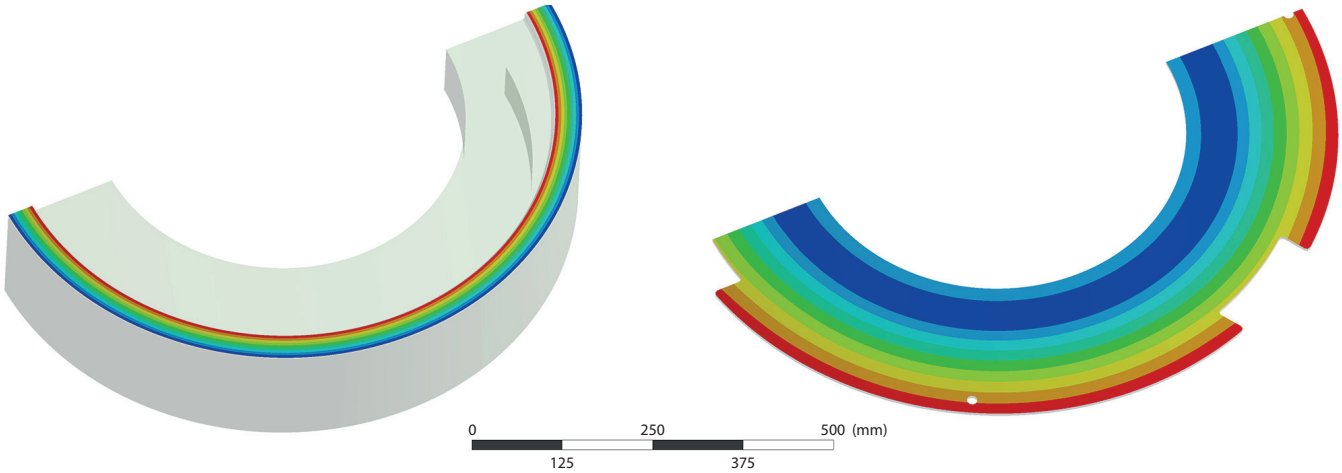

Fig. 10. Results of structural analysis – axial displacement on the measuring surfaces

Fig. 11. Axial stiffness measurement of a single-row ball slewing ring on the test device for large-dimension rolling bearings

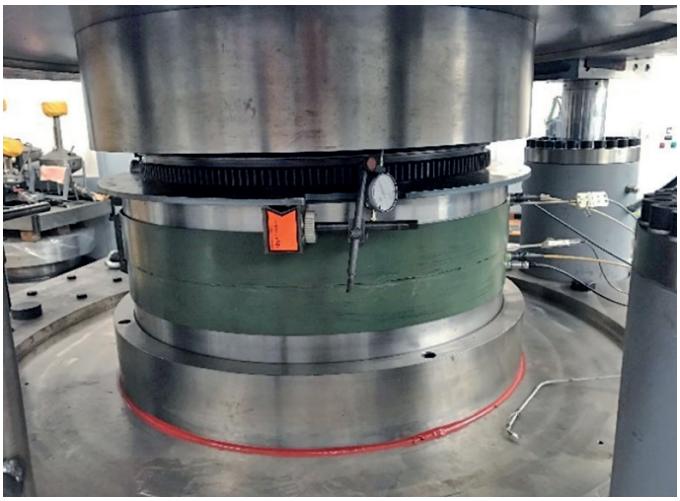

Fig. 12. Positioning of deviation meters along the circumference of the slewing ring being measured

each other between measurements. Values were read from all three deviation meters for each load level. The measured values were averaged and assessed. Figure 13 shows the comparison of axial stiffness characteristics of a single-row ball slewing ring with four-point contact, determined by experimental measurement on the test device and the values calculated by FEM analysis using Ansys/Workbench software on the virtual 3D model. "Irregularities" in the curve obtained by experimental measurement were caused by the impossibility to adjust a precise load value on the test device proportion valve controlling the axial force. Five measurements were made (measured values of displacement at a given load were averaged), these results were compared with an equivalent model using FEM. Figure 13 clearly shows that the axial stiffness characteristics determined by experimental measurement accurately copies the "ideal" characteristics calculated by FEM analysis.

This verification was important due to the correctness of the finite-element analysis setup in order to determine whether the carried-out static structural analysis had correctly defined

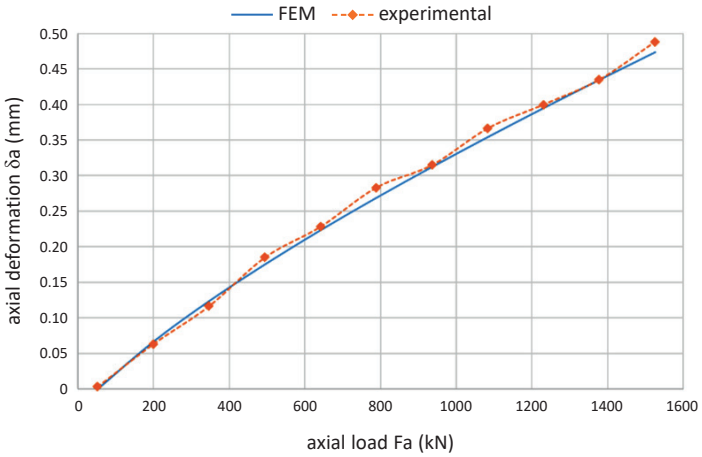

Fig. 13. Comparison of the axial stiffness of a single-row ball slewing ring with four-point contact determined by experimental measurement and calculated by FEM analysis

boundary conditions, adjustment of the contact parameters between the rolling elements and orbital paths, and whether the results obtained from this analysis can be considered relevant.

5. Results

Based on the FEM analysis carried out, and based on the analysis of its results, it can be stated that the magnitude of the constant K (Eq. (9)) is not the same but changes its value with varying slewing parameters. A change in the value of the constant results in a change of the magnitude of the constant c_δ Eq. (12), which can also be called deformation constant.

For the results obtained from the derived Eq. (15) to be as close as possible to reality, the relationship between the magnitude of the constant K was derived, rolling element diameter D_{we} and the slewing ring rolling elements pitch diameter D_{pw}:

$$K = x_1.D_{we}^{x2}.D_{pw} + x_3 D_{we}^{x4}. \tag{16}$$

If the magnitude of the constant K is introduced to Eq. (12), then the magnitude of the deformation constant c_δ will be:

$$c_\delta = \frac{E'}{\left(x_1.D_{we}^{x2}.D_{pw} + x_3.D_{we}^{x4}\right)^{\frac{3}{2}}} * \frac{1}{\left[\frac{2K}{\pi\mu_i}\left(\sum\rho_i\right)^{\frac{1}{3}} + \frac{2K}{\pi\mu_o}\left(\sum\rho_o\right)^{\frac{1}{3}}\right]^{\frac{3}{2}}}. \tag{17}$$

Optimization using genetic algorithms was used to determine the values of parameters x_1 to x_4 (GA Toolbox) in the MathWorks/Matlab software environment (Fig. 14). The objec-

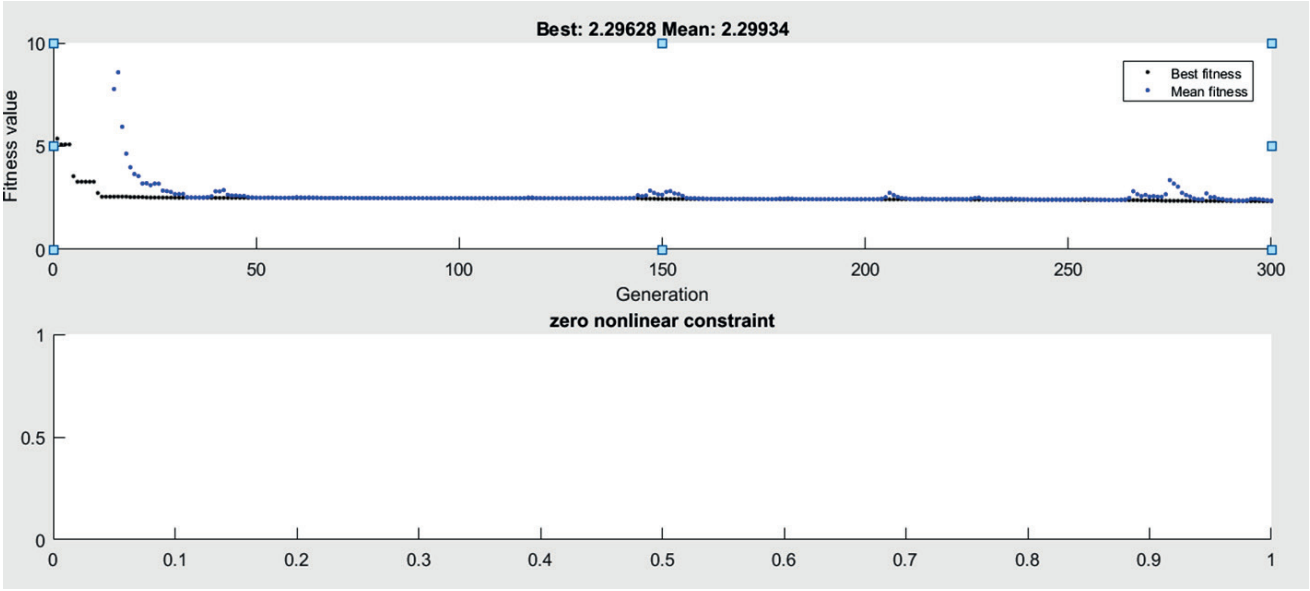

Fig. 14. Optimization of parameters x_1 to x_4 using genetic algorithms in Matlab software environment

tive function (Eq. (18)) for optimization using genetic algorithms was defined as the ratio of the calculated normal force Q_n values according to Eq. (15) and the value calculated by FEM. This ratio was subsequently multiplied by the weight ratio of the maximum value of Q_n and the actual value of Q_i.

$$fx\left(x_1, x_2, x_3, x_4\right) = \sum_{i=1}^{n} \left| \frac{Q_{ni}}{Q_{FEMi}} \right| * \frac{Q_{FEMi}}{Q_{FEM\,\max}}. \qquad (18)$$

Table 2 shows the calculated values of parameters x_1 to x_4 of the constant K for different contact angles α_0 after optimization using genetic algorithms.

Table 2
Values of parameters x_1 to x_4 of the constant K for different contact angles α_0

	x_1	x_2	x_3	x_4
$\alpha_0 = 40°$	0.423879	1.212242	0.381864	0.322300
$\alpha_0 = 45°$	0.406397	1.274663	0.323882	0.334411
$\alpha_0 = 50°$	0.287912	1.255551	0.320456	0.311990
$\alpha_0 = 55°$	0.449431	1.472643	0.369078	0.285915
$\alpha_0 = 60°$	0.154341	1.284813	0.262368	0.389004

Figure 15 shows a comparison of the calculated stiffness characteristics (axial deformation δ_a vs. normal force Q_n acting on a rolling element) analytically according to Eq. (15) after optimization of parameters x_1 to x_4 of the constant K using genetic algorithms (solid lines) with the calculation using the finite-element method (dots). This comparison is only an example of the difference in the calculated values (using the

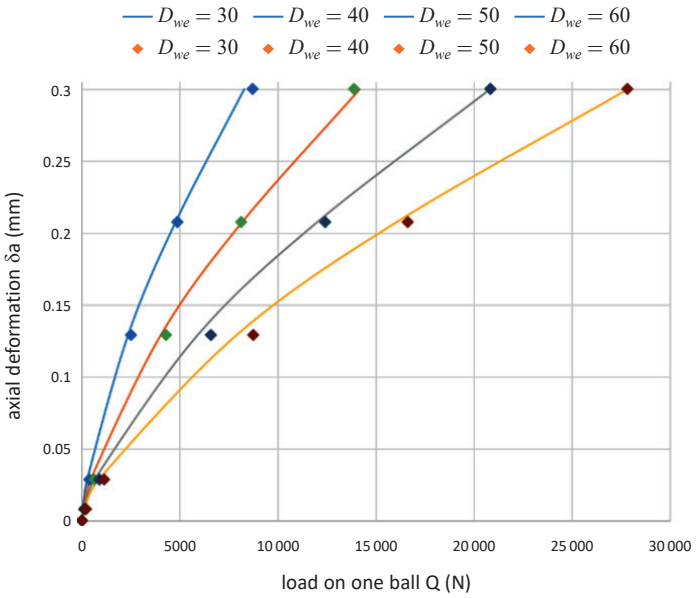

Fig. 15. Axial deformation δ_a vs. normal force Q_n calculated analytically and by FEM

two methods) on a slewing ring with the rolling elements pitch diameter $D_{pw} = 1000$ mm at different diameters D_{we}.

Table 3 lists the calculated values of the constant K for each size of the rolling elements pitch diameter D_{pw} of ball slewing rings in the range from 500 to 1500 mm, for rolling elements diameter D_{we} in the range from 30 to 60 mm, and for contact angle α_0 in the range from 40° to 60°.

Table 4 lists the calculated values of the deformation constant c_δ for each size of the rolling elements pitch diameter D_{pw} of ball slewing rings in the range from 500 to 1500 mm, for the rolling element diameter D_{we} in the range from 30 to 60 mm, and for contact angle α_0 in the range from 40° to 60°.

Table 3
Values of the constant K for different ranges of D_{pw}, D_{we} and α_0

D_{pw} (mm)	500	750	1000	1250	1500
D_{we} (mm)	$\alpha_0 = 40°$				
30	4.575126	6.291270	8.007414	9.723558	11.439702
40	3.675610	4.886481	6.097351	7.308222	8.519093
50	3.195144	4.119032	5.042920	5.966808	6.890696
60	2.910281	3.650964	4.391648	5.132331	5.873014
	$\alpha_0 = 45°$				
30	3.671342	5.001976	6.332611	7.663245	8.993880
40	2.956384	3.878539	4.800695	5.722850	6.645005
50	2.585968	3.279835	3.973703	4.667570	5.361437
60	2.373523	2.923504	3.473484	4.023464	4.573444
	$\alpha_0 = 50°$				
30	2.938017	3.944021	4.950025	5.956028	6.962032
40	2.415014	3.116038	3.817061	4.518085	5.219109
50	2.145468	2.675201	3.204934	3.734667	4.264400
60	1.992263	2.413611	2.834959	3.256307	3.677656
	$\alpha_0 = 55°$				
30	2.476935	3.227403	3.977870	4.728338	5.478805
40	2.042261	2.533556	3.024850	3.516145	4.007439
50	1.836871	2.190566	2.544260	2.897954	3.251649
60	1.730742	2.001152	2.271562	2.541972	2.812381
	$\alpha_0 = 60°$				
30	1.961580	2.449778	2.937975	3.426173	3.914371
40	1.776529	2.113873	2.451217	2.788561	3.125905
50	1.708273	1.961530	2.214788	2.468045	2.721302
60	1.690824	1.891192	2.091560	2.291928	2.492297

Table 4
Values of the deformation constant c_δ for different ranges of D_{pw}, D_{we} and α_0

D_{pw} (mm)	500	750	1000	1250	1500
D_{we} (mm)	$\alpha_0 = 40°$				
30	4.575126	6.291270	8.007414	9.723558	11.439702
40	3.675610	4.886481	6.097351	7.308222	8.519093
50	3.195144	4.119032	5.042920	5.966808	6.890696
60	2.910281	3.650964	4.391648	5.132331	5.873014
	$\alpha_0 = 45°$				
30	3.671342	5.001976	6.332611	7.663245	8.993880
40	2.956384	3.878539	4.800695	5.722850	6.645005
50	2.585968	3.279835	3.973703	4.667570	5.361437
60	2.373523	2.923504	3.473484	4.023464	4.573444
	$\alpha_0 = 50°$				
30	2.938017	3.944021	4.950025	5.956028	6.962032
40	2.415014	3.116038	3.817061	4.518085	5.219109
50	2.145468	2.675201	3.204934	3.734667	4.264400
60	1.992263	2.413611	2.834959	3.256307	3.677656
	$\alpha_0 = 55°$				
30	2.476935	3.227403	3.977870	4.728338	5.478805
40	2.042261	2.533556	3.024850	3.516145	4.007439
50	1.836871	2.190566	2.544260	2.897954	3.251649
60	1.730742	2.001152	2.271562	2.541972	2.812381
	$\alpha_0 = 60°$				
30	1.961580	2.449778	2.937975	3.426173	3.914371
40	1.776529	2.113873	2.451217	2.788561	3.125905
50	1.708273	1.961530	2.214788	2.468045	2.721302
60	1.690824	1.891192	2.091560	2.291928	2.492297

Figures 16 to 19 show nomograms for determining the deformation constant c_δ according to the size of the rolling elements pitch diameter D_{pw} of ball slewing rings, rolling element diameter D_{we} and contact angle α_0.

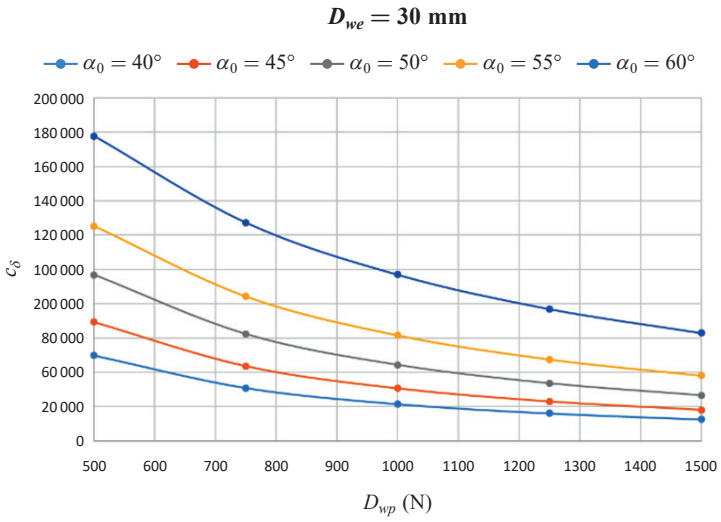

Fig. 16. Nomograms for determining the deformation constant c_δ for the rolling element diameter $D_{we} = 30$ mm

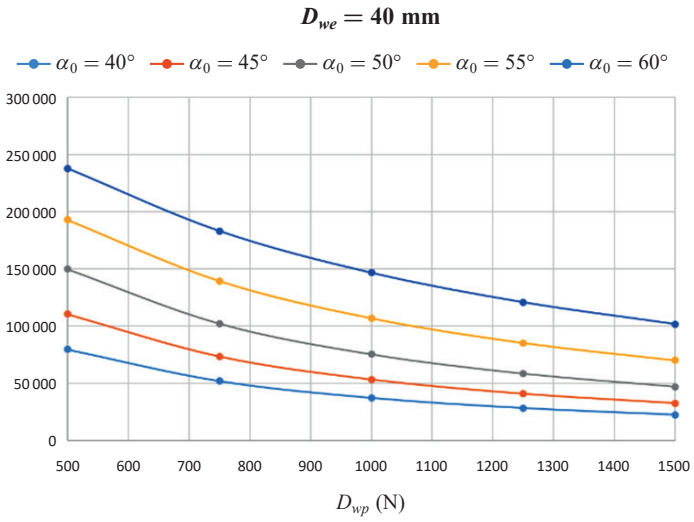

Fig. 17. Nomograms for determining the deformation constant c_δ for the rolling element diameter $D_{we} = 40$ mm

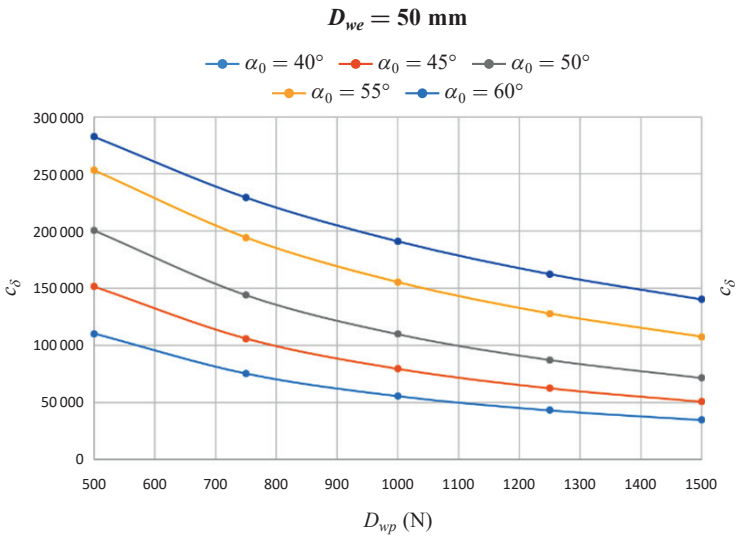

Fig. 18. Nomograms for determining the deformation constant c_δ for the rolling element diameter $D_{we} = 50$ mm

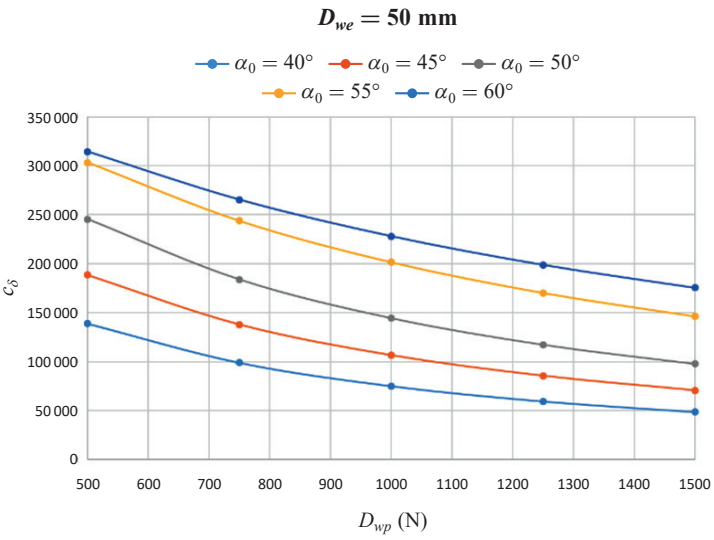

Fig. 19. Nomograms for determining the deformation constant c_δ for the rolling element diameter $D_{we} = 60$ mm

6. Conclusion

This article deals with the design of slewing rings (slewing bearings). Slewing rings are a special type of rolling bearings. They can be considered as large-dimensional ball bearings with angular contact transferring the dominant axial load or tilting moment. The design of slewing rings requires knowing which internal forces act between the rolling elements and the orbital paths, and thus knowing the contact stress state between them.

A fully parametric, 3D virtual model of a ball slewing ring with four-point contact was created in the PTC/Creo Parametric CAD system. This model was subsequently used for finite-element analysis using Ansys/Workbench CAE software. The purpose of FEM analysis was to determine the axial stiffness characteristics (Q_n vs. δ_a). To determine axial stiffness, axial displacement δ_a was evaluated and the magnitude of the force Q_n acting between rolling elements and race orbital paths. Subsequently, the values of δ_a calculated by FEM analysis were used to calculate the deformation constant c_δ in an analytical manner.

The second part of the article describes experimental verification of the slewing ring FEM analysis carried out, in order to determine whether its results conform to reality. For the above purpose, a single-row ball slewing ring with four-point contact was chosen and the following parameters: rolling elements pitch diameter $D_{pw} = 612$ mm, ball diameter $D_{we} = 30$ mm, contact angle $\alpha_0 = 45°$ with raceway curvature ratio $r_i = 0.5186$. After evaluating the results, it was found that the axial stiffness characteristics determined by experimental measurement corresponds to the characteristics calculated by FEM analysis.

The final part of the article describes determination of the auxiliary constant K and deformation constant c_δ for each size of the rolling elements pitch diameter D_{pw} of ball slewing rings in the range from 500 to 1500 mm, for the rolling element diameter D_{we} in the range from 30 to 60 mm, and for contact angle α_0 in the range from 40° to 60°.

Acknowledgements. This study was supported by Slovak Research and Development Agency under the contract no. APVV-14–0508 – Development of new methods for the design of special large-size slewing rings. This study was supported by the Scientific Grant Agency – VEGA no. 1/0595/18 – Optimising the internal geometry of roller bearings with line contact in order to increase their durability and reduce their structural weight.

References

[1] Y. Guo and R.G. Parker, "Stiffness matrix calculation of rolling element bearings using a finite element/contact mechanics model", *Mech. Mach. Theory* 51, 32–45 (2012).

[2] G. Chen and H. Wang, "Contact stress and radial stiffness of a cylindrical roller bearing with corrected roller generator", *Trans. Can. Soc. Mech. Eng.* 40(5), 725–738 (2016).

[3] L. Kania, R. Pytlarz, and S. Spiewak, "Modification of the raceway profile of a single-row ball slewing bearing", *Mech. Mach. Theory* 128, 1–15 (2018).

[4] R. Skyba, S. Hrček, L. Smetanka, and M. Majchrák, "Stiffness analysis of slewing bearings", *IOP Conf. Ser: Mater. Sci. Eng.* 393, 012060 (2018).

[5] P.P. Hou, L.Q. Wang, and Q.Y. Peng, "Vibration analysis of ball bearing considering waviness under high speed and an axial load", *Bull. Pol. Acad. Sci. Tech. Sci.* 68(3), 517–527 (2020).

[6] P. Ding, H. Wang, Y.F. Dai, J. Chen, H. Zhang, and F.Z. Sun, "MDCCS Based Multistage Life Prediction of Slewing Bearing with a Novel Performance Description: an Improved Variational Mode Decomposition Approach", *Exp. Tech.* 43, 341–358 (2019).

[7] Y. Zhang, B. Fang, L. Kong, and Y. Li, "Effect of the ring misalignment on the service characteristics of ball bearing and rotor system", *Mech. Mach. Theory* 151, 103889 (2020).

[8] V.S. Nagarajan, V. Kamaraj, and S. Sivaramakrishnan, "Geometrical sensitivity analysis based on design optimization and multiphysics analysis of PM assisted synchronous reluctance motor", *Bull. Pol. Acad. Sci. Tech. Sci.* 67(1), 155–163 (2019).

[9] E. Kurvinen, J. Sopanen, and A. Mikkola, "Ball bearing model performance on various sized rotors with and without centrifugal and gyroscopic forces", *Mech. Mach. Theory* 90, 240−260 (2015).

[10] G. Chen, G. Wen, Z. Xiao, and H. San, , "Experimental Study on Contact Force in a Slewing Bearing", *J. Tribol.* 140(2), 021402 (2018).

[11] I. Heras, J. Aguirrebeitia, M. Abasolo, and I. Coria, "An engineering approach for the estimation of slewing bearing stiffness in wind turbine generators", *Wind Energy* 22, 376–391 (2018).

[12] T.J. Royston and I. Basdogan, "Vibration transmission through self-aligning (spherical) rolling element bearings", *J. Sound Vibr.* 215, 997–1014 (1998).

[13] F. Bogard, S. Murer, L. Rasolofondraibe, and B. Pottier, "Numerical determination of the mechanical stiffness of a force measurement device based on capacitive probes: Application to roller bearings", *J. Comput. Des. Eng.* 4, 29–36 (2017).

[14] T.L.H. Walford and B.J. Stone, "The measurement of the radial stiffness of rolling element bearings under oscillating conditions", *J. Eng. Mech. Eng. Sci.*22, 175–181 (1980).

[15] R. Tiwari and V. Chakravarthy, "Simultaneous identification of residual unbalances and bearing dynamic parameters from impulse responses of rotor-bearing systems", *Mech. Syst. Signal Proc.* 20, 1590–1614 (2006).

[16] M.J. Goodwin, "Experimental Techniques for bearing impedance measurement", *J. Eng. Ind.* 113(3), 335–342 (1991).

[17] N. Bessous, S. Sbaa, and A.C. Megherbi, "Mechanical fault detection in rotating electrical machines using MCSA-FFT and MCSA-DWT techniques", *Bull. Pol. Acad. Sci. Tech. Sci.* 67(3), 571–582 (2019).

[18] P. He, Y. Wang, H. Liu, E. Guo, and H. Wang, "Optimization design of structural parameters of single-row four-point contact ball slewing bearing", *J. Braz. Soc. Mech. Sci. Eng.* 42, 291 (2020).

[19] J. Brandlein, P. Eschmann, L. Hasbargen, and K. Weigand, *Ball and roller bearings – theory, design and application*, John Wiley&Sons Ltd., 2000.

[20] I. Heras, J. Aguirrebeitia, M. Abasolo, I. Coria, and I. Escanciano, "Load distribution and friction torque in four-point contact slewing bearings considering manufacturing errors and ring flexibility", *Mech. Mach. Theory* 137, 23–26 (2019).

[21] D. Gunia and T. Smolnicki, "The influence of the geometrical parameters for stress distribution in wire raceway slewing bearing", *Arch. Mech. Eng.* 64(3), 315–326 (2017).

[22] A.J. Muminovic, M. Colic, E. Mesic, and I. Saric, "Innovative design of spur gear tooth with infill structure", *Bull. Pol. Acad. Sci. Tech. Sci.* 68(3), 477–483 (2020).

[23] S. Hrček, V. Kraus, R. Kohár, Š. Medvecký, and P. Lehocký, "Construction of a bearing testing apparatus to assess lifetime of large-scale bearings", *Commun: Sci. Lett. Univ. Žilina* 11(2), 57–64 (2009).